



## Tikrit Journal of Pure Science

ISSN: 1813 – 1662 (Print) --- E-ISSN: 2415 – 1726 (Online)

Journal Homepage: <http://tjps.tu.edu.iq/index.php/j>



### Study Of The Structural Properties Of Al-Zn Compounds Manufactured By Powder Technology And Copper-Reinforced

Sukaina Iskandar Yusuf , Sabri Jasim Mohammad, Mohsin Hasan Ali

Physics Department , Collage of Education for pure Science, Tikrit University, Tikrit , Iraq

#### ARTICLE INFO.

##### Article history:

-Received: 31 / 7 / 2023

-Received in revised form: 20 / 8 / 2023

-Accepted: 25 / 8 / 2023

-Final Proofreading: 27 / 1 / 2024

-Available online: 25 / 4 / 2024

**Keywords:** Powder technology, Reinforcement, (Al-Zn) composite, Structural analysis, Crystallinity.

##### Corresponding Author:

**Name:** Sukaina Iskandar Yusuf

**E-mail:**

[Sokayna.e.yussuf@tu.edu.iq](mailto:Sokayna.e.yussuf@tu.edu.iq)

**Tel:**

©2024 THIS IS AN OPEN ACCESS ARTICLE UNDER THE CC BY LICENSE

<http://creativecommons.org/licenses/by/4.0/>



#### ABSTRACT

Due to the importance of aluminium compounds in many industrial fields, therefore, in this study, copper-reinforced (Al-Zn) compounds were prepared in different proportions (0%, 0.4%, 1.2%, and 2%), using the powder technique. The structural properties of the compounds under study were investigated using XRD and EDS tests at room temperature. It was found through the XRD results that the samples were polycrystalline (cubic, tetragonal, monoclinic, and hexagonal). The results of the crystallinity analysis showed that sample (Al-Zn-(0%)Cu) was (12.73%) crystallized, sample (Al-Zn-(0.4%)Cu) was (32.125%) crystallized, sample (Al-Zn-(1.2%)Cu) was (42.771%) crystallized, and sample (Al-Zn-(2%)Cu) was (50.179%) crystallized. Theoretical density of the phases was determined for each sample using independent calculations, taking into consideration some factors such as variations in atomic mass, the number of atoms of the constituent elements, and the size of the unit cell.

### دراسة الخصائص التركيبية لمركبات Al-Zn المصنعة بتقنية المساحيق والمدعمة بالنحاس

سكينة إسكندر يوسف ، صبري جاسم محمد ، محسن حسن علي

قسم الفيزياء ، كلية التربية للعلوم الصرفة ، جامعة تكريت ، تكريت ، العراق

#### الملخص

نظرا لأهمية مركبات الألمنيوم في العديد من المجالات الصناعية، لذا تم في هذه الدراسة، تحضير مركبات (Al-Zn) المقواة بالنحاس بنسب مختلفة (0%، 0.4%، 1.2%، 2%) بوساطة تقنية المساحيق. تم دراسة الخصائص التركيبية للمركبات قيد الدراسة باستخدام فحص XRD و EDS عند درجة حرارة الغرفة. وجد من خلال نتائج XRD أن العينات كانت متعددة البلورات (مكعب، رباعي الزوايا، أحادي الميل، سداسي). أظهرت نتائج تحليل التبلور أن العينة (Al-Zn-(0%)Cu) متبلورة بنسبة (12.73%) والعينة (Al-Zn-(0.4%)Cu) متبلورة بنسبة (32.125%) والعينة (Al-Zn-(1.2%)Cu) متبلورة بنسبة (42.771%) والعينة (Al-Zn-(2%)Cu) متبلورة بنسبة (50.179%). تم حساب الكثافة النظرية للأطوار الناتجة لكل عينة بصورة مستقلة، مع الأخذ في الاعتبار بعض العوامل مثل التغيرات في الكتلة الذرية، وعدد ذرات العناصر المكونة، وحجم خلية الوحدة.

## 1. Introduction

Composites are materials that are made up of two or more different materials, each of which has its own unique set of physical and chemical properties. These composites are often preferred over their individual constituents for a variety of reasons. Recent years have seen a rise in the study of Robotic Materials, composites with built-in capabilities for sensing, actuation, computation, and communication [1]. Aluminum-based alloys have been widely utilized in machinery since the seventeenth century due to their favorable structural, physical, mechanical, and tribological properties, as well as their cost-effective production methods. The specific qualities of an alloy are determined by the chemical composition, which refers to the proportion of alloying components to constituent elements [2]. Alloys composed of aluminum (Al) and zinc (Zn) are extensively employed in several commercial sectors, with notable prevalence in the aerospace and automobile domains. Bronze, brass, and cast iron are among the heavy metals that are commonly utilized in the composition of high-strength alloys. The extensive application of these materials is facilitated by their benefits, including durability, corrosion resistance, and malleability. Alloys possessing the following attributes, namely low density, high strength, high corrosion resistance, multi-phase microstructures, ease of fabrication and forming, low melting point, and ductility, have garnered significant attention. The structural basis is sufficiently grounded [3]. Industrial application of aluminum metal matrix composites has increased in recent decades. Metal, fiber, and ceramic like ( $\text{Al}_2\text{O}_3$ , SiC,  $\text{B}_4\text{C}$ , TiC,  $\text{TiB}_2$  and graphite) increase aluminum alloy mechanical and tribological qualities [4]. Numerous studies have been undertaken to explore the reinforcing of aluminum using different processing techniques, such as utilizing powder-technology, the structural properties of metal matrix composites comprised of  $\text{AlSi}_{12}$  aluminum

alloy reinforced with mullite porous preforms were investigated [5]. Garg P. et al. studied the effect of sintering temperature on the structural and mechanical characteristics of aluminum samples prepared by powder technology and reinforced with graphene powder [6]. G. Anil Kumar et al. conducted an investigation of the structural and mechanical characteristics of  $\text{Al}_{70}\text{Zn}_{30}$  samples that were fabricated using powder technology. These samples were reinforced with  $\text{B}_4\text{C}$  powder and afterwards compared to samples reinforced with equivalent quantities of  $\text{Al}_2\text{O}_3$  and SiC powder [7]. S. Khnsaa investigated the structural, physical, and mechanical properties of powder-processed metallic matrix compounds ( $\text{Al/SiC}$  and  $\text{Al/B}_4\text{C}$ ) [8]. A study used powder metallurgy to incorporate SiC-graphite and GNSs into aluminum matrix composites. Examined composite microstructure and reinforcement dispersion. Ball milling with thin GNSs deformed aluminum particles and introduced flaws into carbonaceous phases. The composite had less grain than graphite because GNSs were evenly distributed [9]. Using powder technology, Alam M. and Motgi B. analyzed the structural and mechanical properties of aluminum samples reinforced with differing proportions of SiC powder and fly ash [10]. This study aimed to explore the structural features of copper-reinforced Al-Zn composites, which had not been previously examined, due to the wide range of applications in which aluminum composites are employed.

## 2. Experimentally

### 2.1. Preparation Method

The composite material's base ingredient was aluminum powder mixed with (10% Zn) powder, while the reinforcing material was Cu powder in different percentages. The research powders' details are listed in Table 1.

**Table 1. Properties of the composite materials**

Material	Purity %	Grain size $\mu\text{m}$	Density $\text{gm/cm}^3$	Melting point $^\circ\text{C}$	Manufacture
Al	99.98	<50	2.70	660.0	china
Zn	99.99	<50	7.14	419.5	china
Cu	99.99	<50	8.94	1085	china

After determining the grain sizes using special sieves, we employed a sensitive electrical balance with an accuracy of (0.0001 gm) to weigh the powders before combining them into the compounds. Table 2 shows the weight ratios used in the study.

**Table 2: The weight ratios used in the study**

Composites	Al	Zn	Cu
M1	90.0%	10%	-----
M2	89.6%	10%	0.4%
M3	88.8%	10%	1.2%
M4	88.0%	10%	2.0%

For (30 minutes), powders were manually combined with concentrated ethanol alcohol (as assistant factor) before being dried in an electric drying furnace at ( $50^\circ\text{C}$ ) for (30 minutes) to remove moisture. The samples were shaped using the one-way pressing technique in a hardened carbon steel mold to produce cylinders with a diameter of (1.4 cm) once the mixing process was completed and a homogenous powder was obtained.

The mixed mixture was inserted in the pressing mold and pressed for (45 seconds) at (5 Ton) to avoid elastic return. Pressing machines were used. The

models were placed on ceramic pieces and gradually heated to the sintering temperature of (540 °C) in an electric oven for two hours, until the particles bonded together, porosity decreased, and mechanical resistance increased. The forms were allowed to slow cool inside the furnace until they reached room temperature.

**3. Results and Discussion**

**3.1. XRD analysis**

XRD analysis of the samples was performed using a (Philips PANalytical X’Pert XRD System) The source consisted of (CuK $\alpha$ ) radiation ( $\lambda = 1.54 \text{ \AA}$ ). Each sample was scanned with a step size of (0.1) in the  $2\theta$  range of (10 - 80), figures (1&2) illustrates the XRD pattern of (Al-Zn) composites with different proportions (0%, 0.4%, 1.2%, 2%)Cu. It was noticed that the formation of the polycrystalline phase was consistent with the powder diffraction file of JCPDS Card as shown in tables 3-6.

The observed peaks can be ascribed to the mean interparticle spacing inside the crystalline domains of the generated phases [11]. The greatest diffraction peak indicates crystalline material, while the lowest

trough between the two peaks indicates amorphous material. The calculation of crystallinity ( $X_c$ ) was determined based on the relative percentages [12]:

$$X_c = \left[ \frac{A_c}{(A_c + A_a)} \right] \cdot 100\% \dots(1)$$

Where:

$A_c$  : The area of crystalline peaks.

$A_a$  : The area of amorphous peaks.

The degrees of crystallinity of samples (Al-Zn-(0%)Cu), (Al-Zn-(0.4%)Cu), (Al-Zn-(1.2%)Cu), and (Al-Zn-(2%)Cu) were (12.730, 32.125, 42.771, and 50.179)%, respectively.

The degree of crystallinity of the samples being examined is observed to increase with the higher percentage of added copper. Consequently, this increase in crystallinity results in an elevation of the X-ray reflection from the crystal planes, as evidenced by the heightened Bragg peaks according to the Scherrer formula [13,14,15]:

$$D_{hkl} = \frac{K\lambda}{\beta_{hkl} \cos\theta} \dots(2)$$

Where  $\beta_{hkl}$  is the half width of  $hkl$  reflection, K is particle shape factor.

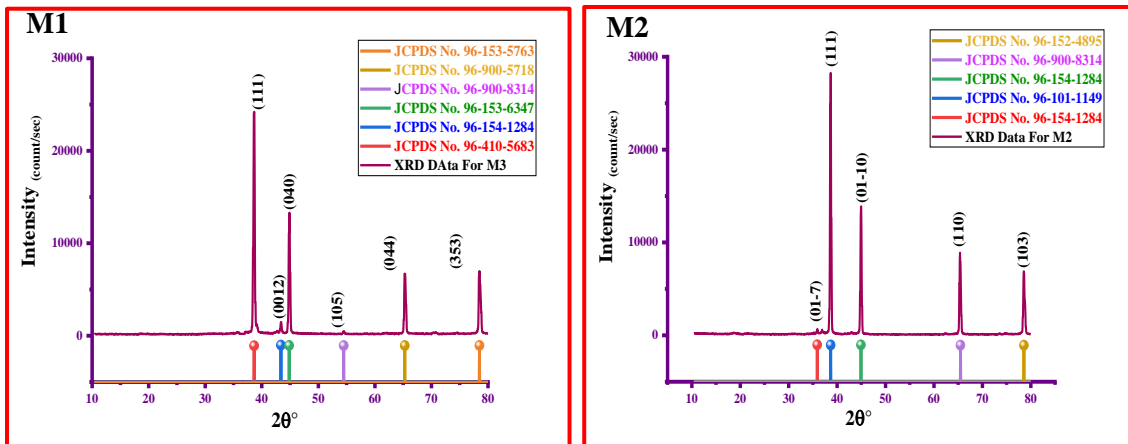


Fig. 1: XRD Data plot of Aluminum composites (Al-Zn-(%)Cu) where: M1 (0%Cu), M2 (0.4%Cu)

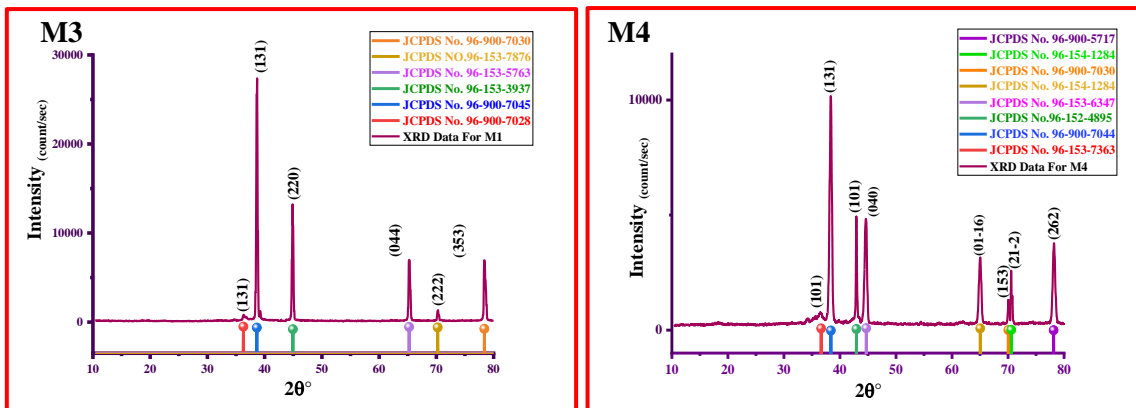


Fig. 2: XRD Data plot of Aluminum composites (Al-Zn-(%)Cu) where: M3 (1.2%Cu) and M4 (2%Cu)

Table 3: XRD test results for (Al-Zn-(0%)Cu) composite

Chemical formula	Crystallite system	2θ degree	d <sub>measured</sub> (Å)	d <sub>standard</sub> (Å)	Rel. Intensities %
Zn <sub>8</sub> Al <sub>16</sub> O <sub>32</sub>	Cubic/Fd-3m/227	36.2699	2.47686	2.40305	2.53
Zn <sub>8</sub> Al <sub>16</sub> O <sub>32</sub>	Cubic/Fd-3m/227	38.6299	2.33080	2.34033	100
Al <sub>10.64</sub> O <sub>16</sub>	Tetragonal/I41/amd/141	44.9376	2.01721	1.99828	42.40
Al <sub>19.2</sub> O <sub>32</sub> Zn <sub>2.4</sub>	Cubic/Fd-3m/227	65.2444	1.42005	1.41421	27.10
O <sub>4</sub> Zn <sub>4</sub>	Cubic/F-43m/216	70.2306	1.34024	1.33628	4.23
Zn <sub>8</sub> Al <sub>16</sub> O <sub>32</sub>	Cubic/Fd-3m/227	78.3696	1.21917	1.21160	26.99

Table 4: XRD test results for (Al-Zn-(0.4%)Cu) composite

Chemical formula	Crystallite system	2θ degree	d <sub>measured</sub> (Å)	d <sub>standard</sub> (Å)	Rel. Intensities %
Al <sub>12.6</sub> Zn <sub>2.1</sub> Cu <sub>9.6</sub>	Hexagonal/R3/146	35.894	2.50193	2.52322	1.96
Cu <sub>4</sub> O <sub>4</sub>	Monoclinic/C12/C1/15	38.6354	2.33048	2.31177	100
Al <sub>12.6</sub> Zn <sub>2.1</sub> Cu <sub>9.6</sub>	Hexagonal/R3/146	44.9543	2.01650	2.04793	56.33
Cu <sub>2</sub> Al <sub>2</sub> O <sub>4</sub>	Hexagonal/P63/mmc/194	65.4389	1.42627	1.42900	31.61
Cu <sub>0.4</sub> Zn <sub>1.6</sub>	Hexagonal/P63/mmc/194	78.5513	1.21680	1.22586	27.88

Table 5: XRD test results for (Al-Zn-(1.2%)Cu) composite

Chemical formula	Crystallite system	2θ degree	d <sub>measured</sub> (Å)	d <sub>standard</sub> (Å)	Rel. Intensities %
Cu <sub>4</sub> O <sub>4</sub>	Monoclinic/C12/C1/15	38.6520	2.32952	2.33946	100
Al <sub>12.6</sub> Zn <sub>2.1</sub> Cu <sub>9.6</sub>	Hexagonal/R3/146	43.4118	2.08450	2.08633	5.39
Cu <sub>8</sub> Al <sub>16</sub> O <sub>32</sub>	Cubic/Fd-3m/227	44.8362	2.02145	2.02150	45.32
Cu <sub>2</sub> Al <sub>2</sub> O <sub>4</sub>	Hexagonal/P63/mmc/194	54.5450	1.68245	1.66837	0.92
Cu <sub>8</sub> Al <sub>16</sub> O <sub>32</sub>	Cubic/Fd-3m/227	65.2896	1.42917	1.42853	27.01
Al <sub>19.2</sub> O <sub>32</sub> Zn <sub>2.4</sub>	Cubic/Fd-3m/227	78.4328	1.21834	1.21999	25.95

Table 6: XRD test results for M4: (Al-Zn-(2%)Cu) composite

Chemical formula	Crystallite system	2θ degree	d <sub>measured</sub> (Å)	d <sub>standard</sub> (Å)	Rel. Intensities %
Al <sub>3</sub> O <sub>6</sub> Cu <sub>3</sub>	Hexagonal/R-3m/166	36.5370	2.45936	2.45316	4.89
Zn <sub>8</sub> Al <sub>16</sub> O <sub>32</sub>	Cubic/Fd-3m/227	38.3740	2.34576	2.34897	100.00
Cu <sub>0.4</sub> Zn <sub>1.6</sub>	Hexagonal/P63/mmc/194	42.9327	2.10665	2.07805	47.95
Cu <sub>8</sub> Al <sub>16</sub> O <sub>32</sub>	Cubic/Fd-3m/227	44.7191	2.02655	2.02150	45.55
Al <sub>12.6</sub> Zn <sub>2.1</sub> Cu <sub>9.6</sub>	Hexagonal/R3/146	65.0176	1.43449	1.43250	29.07
Zn <sub>8</sub> Al <sub>16</sub> O <sub>32</sub>	Cubic/Fd-3m/227	70.0322	1.34355	1.34295	10.81
Al <sub>12.6</sub> Zn <sub>2.1</sub> Cu <sub>9.6</sub>	Hexagonal/R3/146	70.5472	1.33500	1.33795	24.72
Cu <sub>8</sub> Al <sub>16</sub> O <sub>32</sub>	Cubic/Fd-3m/227	78.1294	1.22231	1.21780	31.91

The lattice parameters (a, b, and c) of the cell were determined through X-ray diffraction (XRD) according to the equations [16,17]:

Cubic:

$$\frac{1}{d^2} = \frac{h^2+k^2+l^2}{a^2} \dots (3)$$

Hexagonal:

$$\frac{1}{d^2} = \frac{4}{3} \left( \frac{h^2+hk+k^2}{a^2} \right) + \frac{l^2}{c^2} \dots (4)$$

Monoclinic:

$$\frac{1}{d^2} = \left( \frac{h^2}{a^2} + \frac{k^2 \sin^2 \beta}{b^2} + \frac{l^2}{c^2} - \frac{2hlc \cos \beta}{ac} \right) \csc^2 \beta \dots (5)$$

Tetragonal:

$$\frac{1}{d^2} = \frac{h^2+k^2}{a^2} + \frac{l^2}{c^2} \dots (6)$$

The volume V of the unit cell for the crystal phases was calculated. [13,18,19,20]:

Cubic:

$$V = a^3 \dots (7)$$

Hexagonal:

$$V = \frac{\sqrt{3}}{2} a^2 c \dots (8)$$

Monoclinic:

$$V = abc \sin \alpha \dots (9)$$

Tetragonal:

$$V = a^2 c \dots (10)$$

The theoretical density  $\rho_{x-ray}$  of samples under study was calculated using equation (11) and discovered that the molar mass, which is dependent on the atomic mass and number of elements in the single phase and the unit cell size, changes for each phase [13,16,17]:

$$\rho_{x-ray} = \frac{ZM_{wt.}}{N_A V} \dots (11)$$

Where:

<https://doi.org/10.25130/tjps.v29i2.1493>

Z: Atom's number in unit cell.

$M_{wt.}$ : Molar mass

$N_A$ : number of Avogadro

V: Unit cell volume

Tables 7–10 illustrate the lattice parameters (a, b, and c), the angles ( $\alpha^\circ$ ,  $\beta^\circ$ ,  $\gamma^\circ$ ), the volume V of the unit cell and theoretical densities.

**Table7: Crystallite system characteristic for (Al-Zn-(0%)Cu) composite**

Chemical formula	a (Å)	b (Å)	c (Å)	$\alpha^\circ$	$\beta^\circ$	$\gamma^\circ$	V (Å) <sup>3</sup>	$\rho$ ( $\frac{gm}{cm^3}$ )
Zn <sub>8</sub> Al <sub>16</sub> O <sub>32</sub>	7.970	7.970	7.970	90	90	90	506.26	4.81
Zn <sub>8</sub> Al <sub>16</sub> O <sub>32</sub>	7.762	7.762	7.762	90	90	90	467.65	5.21
Al <sub>10.64</sub> O <sub>16</sub>	5.652	5.652	7.871	90	90	90	251.44	3.59
Al <sub>19.2</sub> O <sub>32</sub> Zn <sub>2.4</sub>	8.000	8.000	8.000	90	90	90	512.00	3.85
O <sub>4</sub> Zn <sub>4</sub>	4.629	4.629	4.629	90	90	90	99.190	5.45
Zn <sub>8</sub> Al <sub>16</sub> O <sub>32</sub>	7.945	7.945	7.945	90	90	90	501.51	4.86

**Table 8: Crystallite system characteristic for (Al-Zn-(0.4%)Cu) composite**

Chemical formula	a (Å)	b (Å)	c (Å)	$\alpha^\circ$	$\beta^\circ$	$\gamma^\circ$	V (Å) <sup>3</sup>	$\rho$ ( $\frac{gm}{cm^3}$ )
Al <sub>12.6</sub> Zn <sub>2.1</sub> Cu <sub>9.6</sub>	4.111	4.111	25.036	90	90	120	366.43	4.93
Cu <sub>4</sub> O <sub>4</sub>	4.653	3.410	5.108	90	99.48	90	79.940	6.61
Al <sub>12.6</sub> Zn <sub>2.1</sub> Cu <sub>9.6</sub>	4.111	4.111	25.03	90	90	120	366.43	4.93
Cu <sub>2</sub> Al <sub>2</sub> O <sub>4</sub>	2.858	2.858	11.293	90	90	120	79.88	5.09
Cu <sub>0.4</sub> Zn <sub>1.6</sub>	2.742	2.742	4.294	90	90	120	27.96	7.72

**Table 9: Crystallite system characteristic for (Al-Zn-(1.2%)Cu) composite**

Chemical formula	a (Å)	b (Å)	c (Å)	$\alpha^\circ$	$\beta^\circ$	$\gamma^\circ$	V (Å) <sup>3</sup>	$\rho$ ( $\frac{gm}{cm^3}$ )
Cu <sub>4</sub> O <sub>4</sub>	4.649	3.438	5.187	90	90	98.64	81.96	6.45
Al <sub>12.6</sub> Zn <sub>2.1</sub> Cu <sub>9.6</sub>	4.111	4.111	25.036	90	90	120	366.43	4.93
Cu <sub>8</sub> Al <sub>16</sub> O <sub>32</sub>	8.086	8.086	8.086	90	90	90	528.69	4.56
Cu <sub>2</sub> Al <sub>2</sub> O <sub>4</sub>	2.858	2.858	11.293	90	90	120	79.88	5.09
Cu <sub>8</sub> Al <sub>16</sub> O <sub>32</sub>	8.081	8.081	8.081	90	90	90	527.71	4.57
Al <sub>19.2</sub> O <sub>32</sub> Zn <sub>2.4</sub>	8.000	8.000	8.000	90	90	90	512.00	3.85

**Table10: Crystallite system characteristic for (Al-Zn-(2%)Cu) composite**

Chemical formula	a (Å)	b (Å)	c (Å)	$\alpha^\circ$	$\beta^\circ$	$\gamma^\circ$	V (Å) <sup>3</sup>	$\rho$ ( $\frac{gm}{cm^3}$ )
Al <sub>3</sub> O <sub>6</sub> Cu <sub>3</sub>	2.8627	2.8627	16.9788	90	90	120	120.5	5.06
Zn <sub>8</sub> Al <sub>16</sub> O <sub>32</sub>	7.790	7.790	7.790	90	90	90	472.73	5.15
Cu <sub>0.4</sub> Zn <sub>1.6</sub>	2.742	2.742	4.294	90	90	120	27.96	7.72
Cu <sub>8</sub> Al <sub>16</sub> O <sub>32</sub>	8.086	8.086	8.086	90	90	90	528.69	4.56
Al <sub>12.6</sub> Zn <sub>2.1</sub> Cu <sub>9.6</sub>	4.111	4.111	25.036	90	90	120	366.43	4.93
Zn <sub>8</sub> Al <sub>16</sub> O <sub>32</sub>	7.945	7.945	7.945	90	90	90	501.51	4.86
Al <sub>12.6</sub> Zn <sub>2.1</sub> Cu <sub>9.6</sub>	4.111	4.111	25.036	90	90	120	366.43	4.93
Cu <sub>8</sub> Al <sub>16</sub> O <sub>32</sub>	8.078	8.078	8.078	90	90	90	527.12	4.57

In figure (3), we see a VESTA drawing depicting the

crystal structure of the phases formed in samples under study.

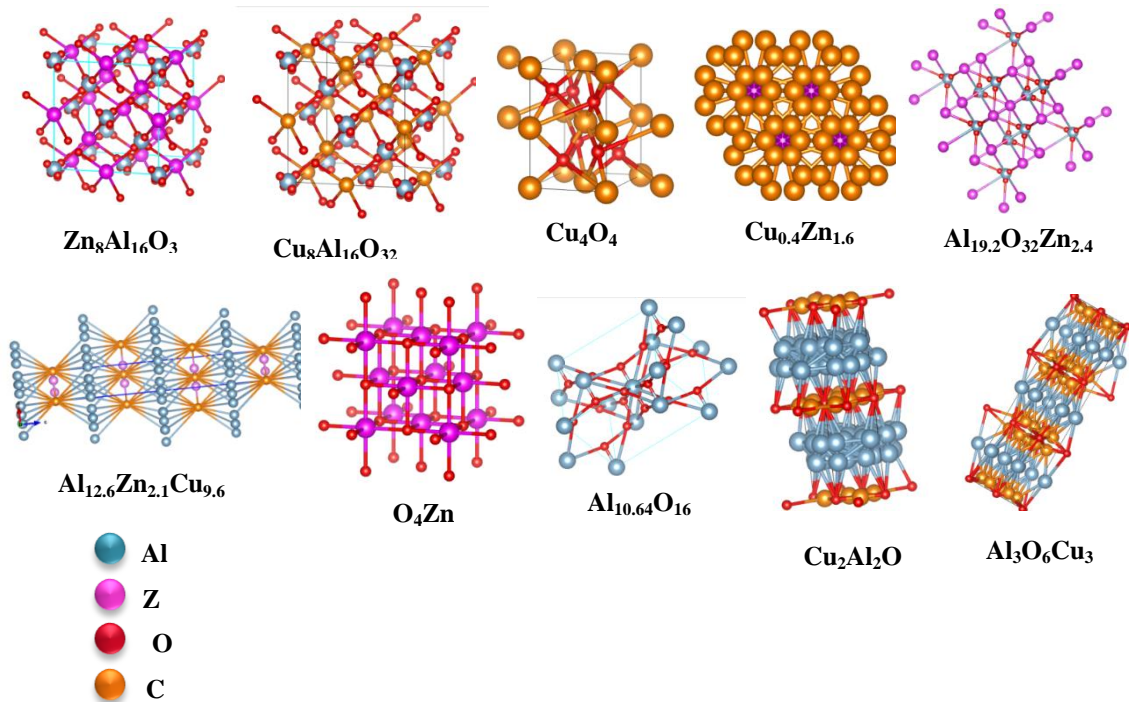


Fig. 3: The crystal structure of the phases generated in the samples under study

### 3.2. EDS analysis

EDS characterization was carried out using a (FESEM system equipped by Oxford instrument in Iran). In order to confirm the (Al-Zn) composites, an

EDS analysis was performed. EDS measurements were focused on a different area and corresponding peaks are shown in the Figures 4-7 and Tables 11-14.

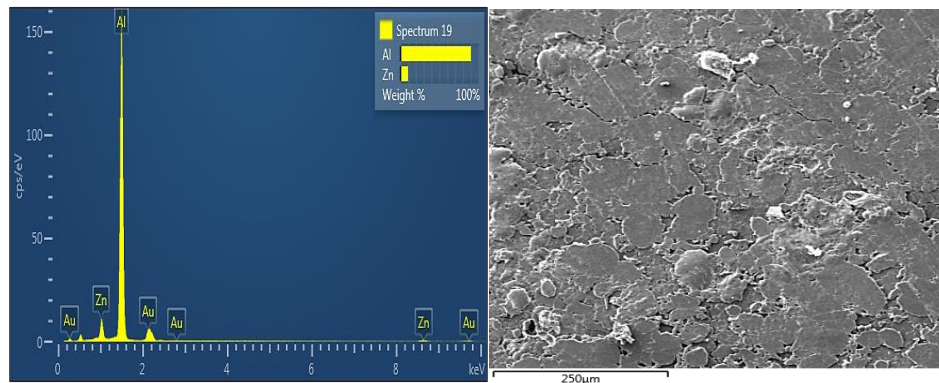


Fig. 4: EDS test plot and FESEM image of (Al-Zn-(%0)Cu) composites

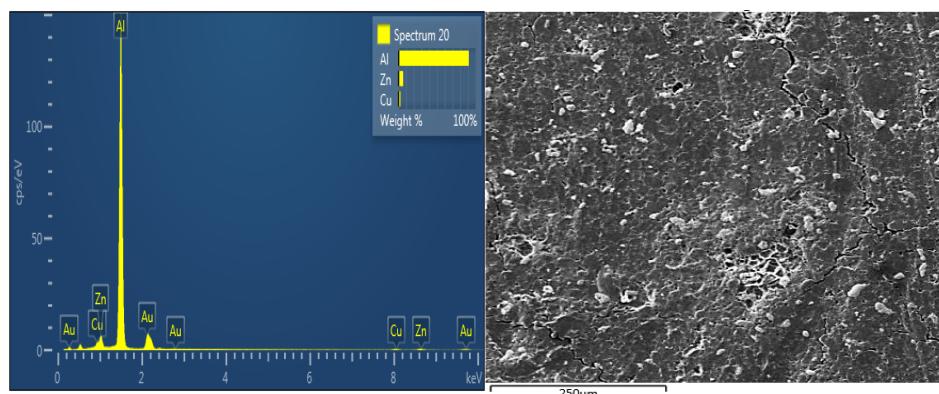


Fig. 5: EDS test plot and FESEM image of (Al-Zn-(%0.4)Cu) composites

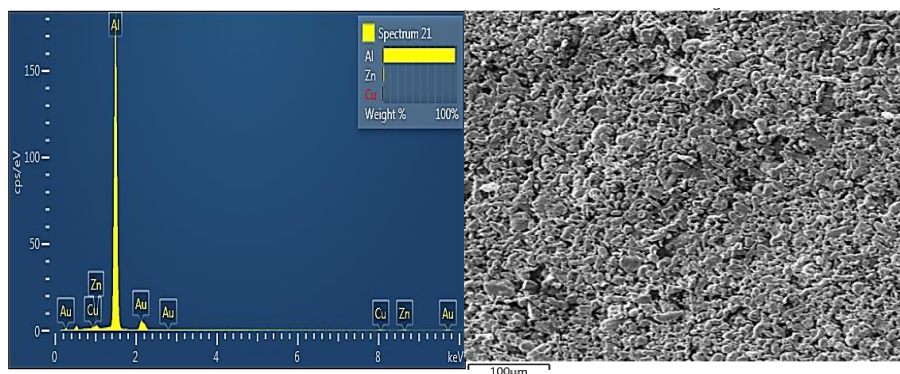


Fig. 6: EDS test plot and FESEM image of (Al-Zn-(%1.2)Cu) composites

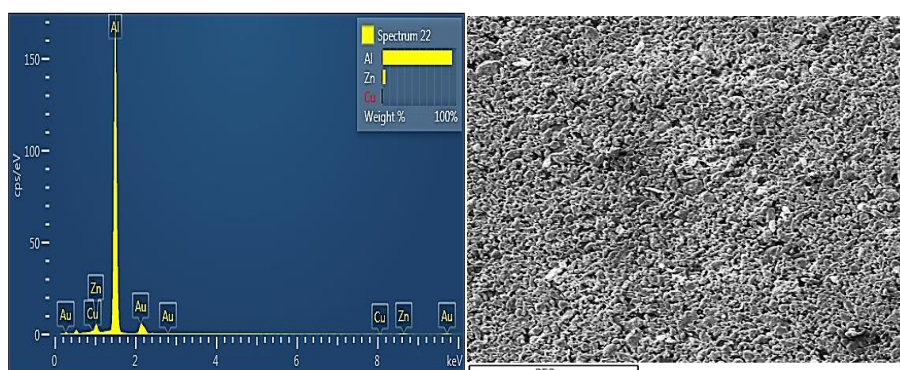


Fig. 7: EDS test plot and FESEM image of (Al-Zn-(%2)Cu) composites

Table 11: Elements analysis of (Al-Zn-(0%)Cu) composite

Element	Line Type	Apparent Concentration	k Ratio	Wt%	Wt% Sigma	Atomic %	Standard Lable	Factory Standard
Al	K-series	20.10	0.14433	90.17	0.26	95.69	Al <sub>2</sub> O <sub>3</sub>	Yes
Zn	L-series	1.49	0.01492	9.83	0.26	4.31	Zn	Yes
Total:				100.00		100.00		

Table 12: Elements analysis of (Al-Zn-(0.4%)Cu) composite

Element	Line Type	Apparent Concentration	k Ratio	Wt%	Wt% Sigma	Atomic %	Standard Lable	Factory Standard
Al	K-series	18.63	0.13383	91.14	0.31	96.11	Al <sub>2</sub> O <sub>3</sub>	Yes
Cu	L-series	0.37	0.00366	2.67	0.24	1.19	Cu	Yes
Zn	L-series	0.80	0.00803	6.20	0.22	2.70	Zn	Yes
Total:				100.00		100.00		

Table 13: Elements analysis of (Al-Zn-(1.2%)Cu) composite

Element	Line Type	Apparent Concentration	k Ratio	Wt%	Wt% Sigma	Atomic %	Standard Lable	Factory Standard
Al	K-series	22.74	0.16330	97.14	0.26	98.79	Al <sub>2</sub> O <sub>3</sub>	Yes
Cu	L-series	0.16	0.00159	1.08	0.19	0.47	Cu	Yes
Zn	L-series	0.26	0.00256	1.78	0.17	0.75	Zn	Yes
Total:				100.00		100.00		

Table 14: Elements analysis of (Al-Zn-(2%)Cu) composite

Element	Line Type	Apparent Concentration	k Ratio	Wt%	Wt% Sigma	Atomic %	Standard Lable	Factory Standard
Al	K-series	21.47	0.15418	94.55	0.28	97.67	Al <sub>2</sub> O <sub>3</sub>	Yes
Cu	L-series	0.09	0.00092	0.62	0.21	0.27	Cu	Yes
Zn	L-series	0.70	0.00699	4.82	0.20	2.06	Zn	Yes
Total:				100.00		100.00		

#### 4. Conclusions

Aluminum compounds are essential in many fields due to their characteristics. Some of them were made and studied in this study. The XRD analysis of the powder metallurgy-prepared samples under study

revealed the following about their structural properties: Crystal systems observed in samples under study include (cubic, tetragonal, monoclinic, and hexagonal), indicating that the material is polycrystalline. The results of the crystallinity

<https://doi.org/10.25130/tjps.v29i2.1493>

analysis showed that sample (Al-Zn-(0%)Cu) was (12.730%) crystallized, sample (Al-Zn-(0.4%)Cu) was (32.125%) crystallized, sample (Al-Zn-(1.2%)Cu) was (42.771%) crystallized, and sample (Al-Zn-(2%)Cu) was (50.179%) crystallized. Theoretical density of the phases was determined for

## References

- [1] Kumar G.K., Sankar C., 2019, *Mechanical Behaviour of Silicon Carbide(Sic) / Fly Ash particles Reinforced Aluminium-7075 Based Metal Matrix Composite Fabricated By Stir Casting Method*, *IJSART*, 5:2.
- [2] Hekimoğlu A. P., Turan Y. E., İsmailoğlu İ. İ., Akyol M. E., Şen E., 2019, *Bor ile yapılan tane inceltmenin Al-30Zn alaşımının mikroyapı ve mekanik özelliklerine etkisi*, *Journal of the Faculty of Engineering and Architecture of Gazi University*, 34:1 , 523-534.
- [3] Balamugundan B, Karthikeyan L, Karthik K and Keerthi C., 2017. *Enhancement of mechanical properties on Aluminum alloys- A review. IOSR Journal of Mechanical and Civil Engineering (IOSR JMCE):2320–2340.*
- [4] Savaskan T., Alemdağ Y., 2010, *Effect of nickel additions on the mechanical and sliding wear properties of Al-40Zn- 3Cu alloy*, *Wear*, 268, 565-570.
- [5] Tomiczek B., Kujawa M., Matula G., Kremzer M., Tański T., Dobrzański L. A., 2015, *Aluminium AlSi12 alloy matrix composites reinforced by mullite porous preforms*, *Material science & engineering technology*, Volume46, Issue4-5.
- [6] Garg P., Gupta P., Kumar D., Parkash O., 2016, *Structural and Mechanical Properties of Graphene reinforced Aluminum Matrix Composites*, *J. Mater. Environ. Sci.*, 7:5 ,1461-1473.
- [7] Kumar G., Sateesh J. , Kumar Y. T., Madhusudhan T., 2016, *Properties of Al7075-B4C Composite prepared by Powder Metallurgy Route*, *International Research Journal of Engineering and Technology (IRJET)*, 03:07.
- [8] Salman K., 2017, *Comparison the Physical and Mechanical Properties of Composite Materials (Al /SiC and Al/ B4C) Produced by Powder Technology*, *Journal of Engineering*, 10:23.
- [9] Zhang, J., Liu, Q., Yang, S., Chen, Z., Liu, Q. & Jiang, Z., 2020, *Microstructural evolution of hybrid aluminum matrix composites reinforced with SiC nanoparticles and graphene/graphite prepared by powder metallurgy*, *Progress in Natural Science: Materials International*, 30:2, 192-199.
- [10] Alam M., Motgi B., 2021, *Study on Microstructure and Mechanical Properties of Al7068 Reinforced with Silicon Carbide and Fly Ash by Powder Metallurgy*, *International Journal for Modern Trends in Science and Technology*, 7(09): 47-53.
- [11] Abdullah O. Gh., Aziz Sh. B., Rasheed Mariwan A., 2016, *Structural and optical characterization of PVA:KMnO4 based solid polymer electrolyte*, *Results in Physics*, Volume 6, Pages 1103-1108.
- [12] Aziz Sh. B., Abdullah O. Gh, Rasheed M. A., Ahmed H. M., 2017, *Effect of High Salt Concentration (HSC) on Structural Morphological, and Electrical Characteristics of Chitosan Based Solid Polymer Electrolytes*, *Polymers*, 9, 187.
- [13] Yusuf S. I., Meteab M. M., Annaz A. A., 2022, *Crystal Diffraction Techniques Were Used to Investigate the Structural Properties of Some Aluminum Alloys. , IOP Conf. Series: Earth and Environmental Science 961 (2022,) 012018.*
- [14] Bokuniaeva A. O., Vorokh A. S., 2019, *Estimation of particle size using the Debye equation and the Scherrer formula for polyphasic TiO2 powder*, *Journal of Physics: Conference Series 1410* , 012057, IOP Publishing.
- [15] Tirpude M. P., .Tayade N. T., 2022, *Frustrate microstructures composed PbS cluster's size perspective from XRD by variant models of Williamson-Hall plot method*, *Research Article*, Version 1, DOI: <https://doi.org/10.21203/rs.3.rs-1586320/v1> .
- [16] Jasem I. K., Abdul-Aziz A.F., Ibrahim N.M., 2018, *Fabrication and study of the structural and spectral properties of the composites (y) Mn<sub>0.6</sub> Zn<sub>0.4</sub> Fe<sub>2</sub>O<sub>4</sub> + (1-y) PZT prepared by the powder technology method*, *Tikrit Journal of Pure Science*, 23 (10).
- [17] Abdul-Aziz A.F, 2016, *Study structural, dielectric and ferroelectric properties of Pb (Zr<sub>1-x</sub> Ti<sub>x</sub>)O<sub>3</sub> ceramics near the morphotropic phase boundary*, *Tikrit Journal of Pure Science*, 21 (3).
- [18] Augustin M., Balu T., 2017, *Estimation of Lattice Stress and Strain in Zinc and Manganese Ferrite Nanoparticles by Williamson-Hall and Size-Strain Plot Method*, *International Journal of Nanoscience* , 16 : 03.
- [19] Kushwaha P., Chauhan P., 2021, *Microstructural evaluation of iron oxide nanoparticles at different calcination temperature by Scherrer, Williamson-Hall, Size-Strain Plot and Halder-Wagner methods*, *Phase Transitions A Multinational Journal*, 94:10, 731–753.
- [20] Wasly H. S., 2018, *X-ray analysis for determination the crystallite size and lattice strain in ZnO nanoparticles*, *Journal Of Al Azhar University Ngeenring Sector*, 13: 49, 1312-1320.